Geometrically Based Statistical Channel Model for Macrocellular Mobile Environments*

Paul Petrus† Jeffrey H. Reed and Theodore S. Rappaport
Mobile and Portable Radio Research Group (MPRG)
Virginia Polytechnic Institute and State University, Blacksburg, USA.
Tel. No. (540) 231-2964, Fax No. (540) 231-2968, email: petrus@sol.mprg.ee.vt.edu

Abstract- **In this paper, we develop a statistical geometric propagation model for a macrocell mobile environment that provides the statistics of angle-of-arrival of the multipath components. This channel model assumes that each multipath component of the propagating signal undergoes only one bounce traveling from the transmitter to the receiver and that scattering objects are located uniformly within a circle around the mobile. This Geometrically Based Single Bounce Macrocell (GBSBM) channel model provides three important parameters that characterize a channel: the power of the multipath components, the time-of-arrival (TOA) of the components, and the angle-of-arrival (AOA) of the components. Doppler spectra and fading envelopes obtained using the GBSBM model is compared with Clarke's model. The results show that the rate of fading at the base station is lower than at the mobile and the reduction in the Doppler spread at the base station is dependent on the direction of motion of the mobile with respect to the base station and the radius of the scattering circle.**

I. Introduction

The recent tremendous growth in wireless communications has led to crowding of the radio spectrum. Traditionally, cell splitting has been employed to cope up with the increase in the number of users in a cellular system. But cell splitting is expensive and requires reconfiguring the cellular network. Therefore, adaptive arrays are currently being investigated for cellular and personal communications to increase the capacity of a cell. Various adaptive array algorithms have been proposed for cellular applications [1, 2, 3]. To test these algorithms using simulation, statistical channel models, which provides the angle-of-arrival (AOA) and time-of-arrival (TOA) of the multipath components, are required.

Classically, dense scattering is viewed as leading to a Rayleigh fading phenomenon for narrowband signals [4]. This model (Clarke's) assumes that the signals arrive horizontally at the receiver antenna and uniformly along the azimuthal coordinate. Aulin proposed a channel model [5] which takes into account the elevation coordinate and which assumes uniform AOAs along the azimuthal coordinate. Aulin's model is appropriate to model fading at a mobile unit, because scatterers are located close to the mobile and are of different heights. Also the scatterers are assumed to be uniformly located around the mobile and therefore the AOAs along the azimuth can be assumed to be uniform. But this model is not appropriate to model signals arriving at the base station. Liberti and Rappaport [6] developed a statistical channel model for microcells called the Geometrically Based Single Bounce model (GBSB). The GBSB model assumes that the scatterers lie in an ellipse which encompasses the transmitter and the receiver.

In this paper, we develop a statistical channel model for macrocells called the Geometrically Based Single Bounce Macrocell (GBSBM)[1] channel model that assumes that multipath reflection is caused by scatterers located close to the mobile. The GBSBM model assumes that the plane waves arrive horizontally at the base station. From this model, the probability density function of the AOA along the azimuth can be computed. The assumption that the plane waves arrive horizontally is valid for macrocellular environment, since the separation of the mobile and the base station is larger than the difference in the height of the base station antenna and the mobile antenna and the scatterers.

The paper is organized as follows: Section II discusses the GBSBM channel model and the derivation of the probability density function (pdf) of angle of arrival of the multipaths at the base station from a mobile surrounded by scatterers. Section III compares theoretical and simulated results of the pdf of the AOA of the multipath components. The Doppler spectrum and the fading envelopes generated using GBSBM model are compared with the Clarke's model in Section IV, and Section V presents the conclusions.

II. Geometrically Based Single Bounce Macrocell (GBSBM) Channel Model

Here we introduce a geometrically based statistical macrocell

*This work was sponsored by the MPRG affiliates program and the Federal Highway Research Center for Excellence at Virginia Tech.

†Point of contact.

[1]The name GBSBM was derived from Liberti's channel model.

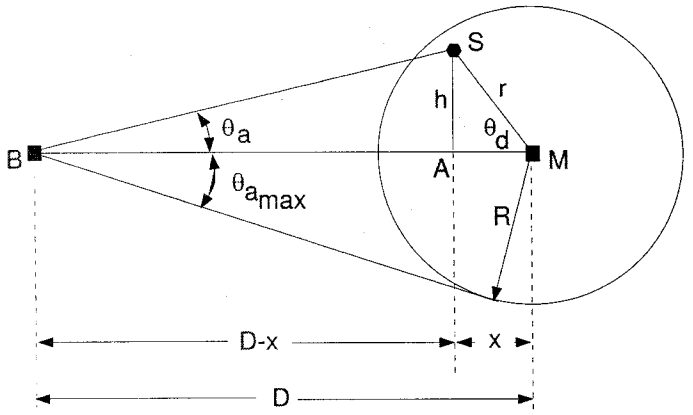

Figure 1: Illustration of the Geometrically Based Single Bounce Macrocell channel (GBSBM) model.

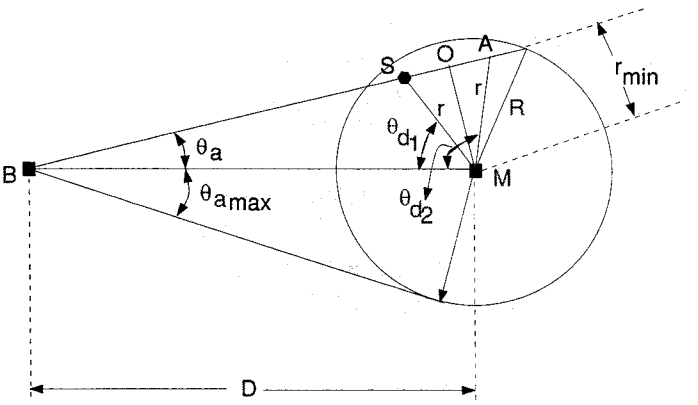

Figure 2: Illustration of the limits of the variable r.

channel model and derive the probability density function of the angle of arrival of the multipath components in a macrocell at the base station. The following are the assumptions made in developing the model:

- The signals received at the base station are assumed to be plane waves arriving from the horizon and hence the angle of arrival calculation includes only the azimuthal coordinate.
- The scatterers are assumed to be uniformly distributed within a circle around the mobile.
- We use the same assumption as in [7], where each scatterer is assumed to be an omnidirectional re-radiating element whereby the plane wave, on arrival, is reflected directly to the mobile receiver antenna without the influence from other scatterers.
- The scatterers are assigned equal scattering coefficients with uniform random phases.

Figure 1 illustrates the GBSBM channel model. The base station is marked as B and M is the mobile unit. The base station and the mobile unit are separated by a distance D. The location of the scatterer is marked as S. The scatterers are assumed to be uniformly located around the mobile inside a circle of radius R. The angle of arrival of the multipath at the base station θ_a from S is dependent on two variables: the angle (θ_d) and the radius (r) of the location of the scatterer S with respect to the mobile unit M. The maximum angle of the arrival ($\theta_{a_{max}}$) of the multipath component is given by

$$\theta_{a_{max}} = arcsin\left(\frac{R}{D}\right). \tag{1}$$

Consider the triangles BAS and AMS, it can be shown that

$$tan(\theta_a) = \frac{rsin(\theta_d)}{(D - rcos(\theta_d))}. \tag{2}$$

Since the scatterers are assumed to be uniformly distributed around the mobile, the probability density function of θ_d is a uniform distribution from 0 to 2π, i.e., $f_{\theta_d}(\theta_d) = \frac{1}{2\pi}, 0 \leq \theta_d \leq 2\pi$. The probability density function of θ_a can be calculated as follows:

- The joint probability density function of θ_a and r, $f_{\theta_a,r}(\theta_a, r)$ is calculated as $f_{\theta_a,r}(\theta_a, r) = f_{\theta_a,r}(\theta_a|r)f_r(r)$.
- The marginal probability density function $f_{\theta_a}(\theta_a)$ is then calculated as $f_{\theta_a}(\theta_a) = \int_r f_{\theta_a,r}(\theta_a, r)dr$.

The conditional probability density function of the angle of arrival θ_a given r can be evaluated using the following transformation [8].

$$f_{\theta_a,r}(\theta_a|r) = \left.\frac{f_{\theta_d}(\theta_d)}{\left|\frac{dg(\theta_d)}{d\theta_d}\right|}\right|_{\theta_d = g^{-1}(\theta_a)} \tag{3}$$

To calculate the above conditional probability, θ_d has to be expressed as a function of θ_a. This can be achieved by squaring Eqn. 2 and solving the quadratic equation in $cos(\theta_d)$. Squaring Eqn. 2 and solving for θ_d

$$\theta_d = arccos\left[\frac{D}{r}sin^2(\theta_a) \pm \frac{cos(\theta_a)}{r}\sqrt{r^2 - D^2sin^2(\theta_a)}\right]. \tag{4}$$

Differentiating Eqn. 2,

$$\frac{d\theta_a}{d\theta_d} = \frac{(Drcos(\theta_d) - r^2)}{sec^2(\theta_a)(D - rcos(\theta_d))^2}. \tag{5}$$

Using Eqns. 3 and 5, the conditional probability density function of the angle of arrival θ_a given r is given by

$$f_{\theta_a,r}(\theta_a|r) = \frac{1}{2\pi}\left|\frac{sec^2(\theta_a)(D - rcos(\theta_d))^2}{(Drcos(\theta_d) - r^2)}\right|, \tag{6}$$

where θ_d is given by Eqn. 4. Considering that the users are uniformly distributed in a cell, the joint probability density

function of θ_d and r is given by [6]

$$f_{\theta_d,r}(\theta_d,r) = \frac{r}{\pi R^2} \tag{7}$$

and is also equal to $f_r(r)f_{\theta_d}(\theta_d)$, since r and θ_d are independent random variables. The probability density function of r is then given by $f_r(r) = \frac{f_{\theta_d,r}(\theta_d,r)}{f_{\theta_d}(\theta_d)}$, where $f_{\theta_d}(\theta_d) = 1/2\pi$. Therefore,

$$f_r(r) = \frac{2r}{R^2}. \tag{8}$$

The marginal probability density function $f_{\theta_a}(\theta_a)$ is then given by

$$f_{\theta_a}(\theta_a) = \frac{1}{\pi R^2}\int_r \left|\frac{sec^2(\theta_a)\,[D - rK]^2}{[DK - r]}\right| dr, \tag{9}$$

where

$$K = \frac{D}{r}sin^2(\theta_a) \pm \frac{cos(\theta_a)}{r}\sqrt{r^2 - D^2 sin^2(\theta_a)}.$$

Now we evaluate the limits of the variable r. Figure 2 illustrates the limits of the random variable r. For a particular value θ_a, r ranges from a minimum of r_{min} to a maximum of R. From Figure 2, it can be seen that r_{min} is the length of the perpendicular line from M to the line BA. It can also be seen that for a particular value of r, there are two possible values of θ_d, i.e., θ_{d_1} and θ_{d_2}. To evaluate the marginal probability density function $f_{\theta_a}(\theta_a)$, the integral has to be split into two parts, where the first integral is integrated with the integrand as a function of θ_{d_1} and the second as a function of θ_{d_2}. The marginal probability density function $f_{\theta_a}(\theta_a)$ is then given by

$$f_{\theta_a}(\theta_a) = \frac{1}{\pi R^2}\left[\int_{r_{min}}^{R}\left|\frac{sec^2(\theta_a)(D - rcos(\theta_{d_1}))^2}{(Dcos(\theta_{d_1}) - r)}\right| dr + \int_{r_{min}}^{R}\left|\frac{sec^2(\theta_a)(D - rcos(\theta_{d_2}))^2}{(Dcos(\theta_{d_2}) - r)}\right| dr\right]. \tag{10}$$

From Figure 2, $r_{min} = Dsin(\theta_a)$, and for every value of θ_{d_1}, the corresponding value of θ_{d_2} is given by $\theta_{d_2} = \theta_{d_1} + 2arccos\left(\frac{r_{min}}{r}\right)$. Therefore Eqn. 10 becomes

$$f_{\theta_a}(\theta_a) = I_1 + I_2, \tag{11}$$

where
$I_1 = \frac{1}{\pi R^2}\left[\int_{r_{min}}^{R}\left|\frac{sec^2(\theta_a)[D-rK]^2}{[DK-r]}\right| dr\right]$,
and
$I_2 = \frac{1}{\pi R^2}\left[\int_{r_{min}}^{R}\left|\frac{sec^2(\theta_a)\left[D-rcos\left(cos^{-1}[K]+2cos^{-1}\left(\frac{r_{min}}{r}\right)\right)\right]^2}{\left[Dcos\left(cos^{-1}[K]+2cos^{-1}\left(\frac{r_{min}}{r}\right)\right)-r\right]}\right| dr\right]$.

The closed form expression for the Eqn. 11 is not tractable and hence the integral is evaluated using numerical integration. But an approximate closed form pdf for the AOA of the multipaths which closely fits the true pdf will be beneficial for further analysis. A closed form expression which fits closely the true pdf is given by

$$f_{\theta_a}(\theta_a) = \begin{cases} \frac{\pi}{4.9\theta_{a_{max}}}cos\left(\frac{\pi}{2}\frac{\theta_a}{\theta_{a_{max}}}\right)^{0.475} & , \quad -\theta_{a_{max}} \le \theta_a \le \theta_{a_{max}} \\ 0 & , \quad otherwise, \end{cases} \tag{12}$$

where θ_a and $\theta_{a_{max}}$ are in degrees. In the next Section, the true pdf of the AOA is compared with the approximate pdf and the simulated normalized histogram.

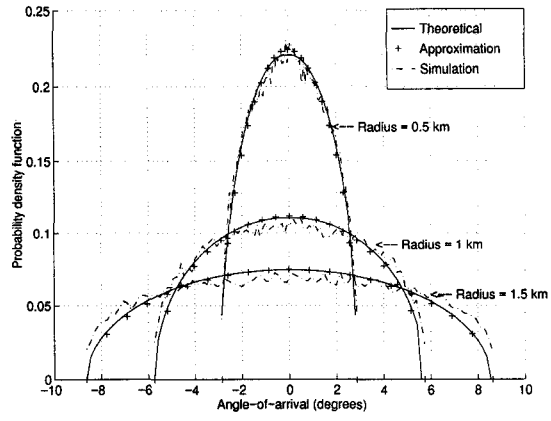

Figure 3: Probability density function for the angle of arrival of the multipath components at the base station from a mobile located 10 km away from the base station and the radii of the scattering circles are 0.5, 1, and 1.5 km.

III. Comparison Of Theoretical And Simulation Results

In this Section, we validate the theoretical model developed in Section II using simulation and compare it with the approximate pdf. The true probability density function in Eqn. 11 is evaluated using numerical integration for a case where the distance of separation between the base station and the mobile unit is 10 km. The scatterers are uniformly located within circles of radii 0.5, 1, and 1.5 km. Simulated normalized histograms are generated by creating uniformly located scatterers by using the pdf in Eqn. 7. For each location of the scatterer, the angle-of-arrival of the signal at the base station B is calculated using Eqn. 2. The histogram for the AOA is then calculated by placing 10,000 scatterers for each radius under consideration. The approximate pdf is calculated using Eqn. 12 where $\theta_{a_{max}}$ is given by Eqn. 1. The normalized histograms, the approximate and the theoretical pdfs are plotted in Figure 3. The simulated histograms and the approximated pdfs match closely the theoretical pdfs. It can be seen that the range of AOA of the multipath components is limited by radius of the scattering circle. The range of AOA of the multipath components increases as the radius of the scattering circle increases. In the limiting case, as the

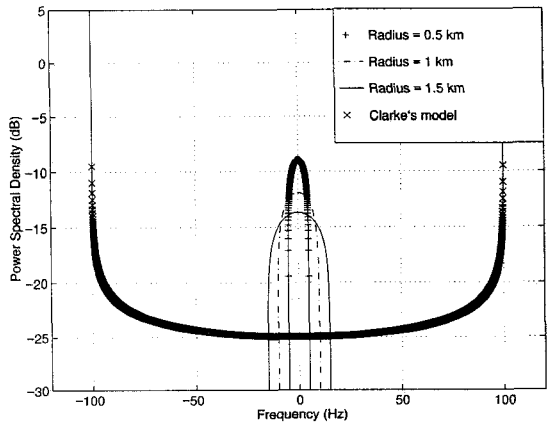

Figure 4: Doppler spectra using the GBSBM model is compared with the Clarke's model. The base station is located 10 km away from a mobile and the radii of the scattering circle are 0.5, 1, and 1.5 km. The motion of the mobile is 90 degrees with respect to the direct component and is traveling at 54 kmph. The carrier frequency is 2 GHz.

radius of the scattering circle tends to zero, there will be no multipath components and hence no fading.

IV. Doppler Spectra And Fading Envelope

The received signal at the base station experiences Doppler spread because of the moving transmitter. The multipath components at the receiver experiences Doppler shift depending on the direction of the motion of the mobile. The ith multipath component experiences a Doppler shift v_i given by

$$v_i = f_m cos(\phi_i - \phi_v), \tag{13}$$

where f_m is the maximum possible Doppler shift which is given by $f_m = v/\lambda$, ϕ_i is the angle between the ith multipath component and the direct path, and ϕ_v is the angle between the direction of the motion of the vehicle and the direct path. Let the baseband complex representation of the received signal be $r(t) = E_o \sum_{i=0}^{L-1} \alpha_i e^{j2\pi v_i t}$, where α_i is the complex multipath amplitude for multipath component i. The Doppler spectrum $S_r(f)$ was shown in [9] to be $S_r(f) = A_o^2 f_v(f)$, where $A_o^2 = E_o^2/4 \sum_{i=1}^{L-1} |\alpha_i|^2$, and $f_v(f)$ is the probability density function of the distribution of the Doppler frequency. Assuming an omnidirectional antenna at the receiver, it was shown in [9] that $f_v(f)$ is given by

$$f_v(f) = \frac{f_\phi(\phi_v + |arccos(v/f_m)|)}{f_m\sqrt{1-(v/f_m)^2}} + \frac{f_\phi(\phi_v - |arccos(v/f_m)|)}{f_m\sqrt{1-(v/f_m)^2}}, |v| < f_m, \tag{14}$$

where $f_\phi(\phi)$ is the pdf of the AOA of the multipath components at the base station which is given by Eqn. 10. Therefore the power spectral density is given by [10]

$$S_r(f) = \frac{A_o^2}{f_m\sqrt{1-(v/f_m)^2}} [f_\phi(\phi_v + |arccos(v/f_m)|) + f_\phi(\phi_v - |arccos(v/f_m)|)], |v| < f_m. \tag{15}$$

The conventional Doppler spectrum is given by Clarke's model [10] as

$$S_r(f) = \frac{A_o^2}{\pi f_m\sqrt{1-(v/f_m)^2}}, |v| < f_m. \tag{16}$$

Table 1: Simulation parameters for the test case in Fig. 5.

Parameters	Values
Carrier frequency	2 GHz
TR separation	10 km
Radii of the scattering circles	0.5, 1, 1.5 km
Velocity of the mobile	33.5 mph
Maximum Doppler frequency	100 Hz
ϕ_v	90 degrees

Consider a test case whose parameters are listed in Table 1. The mobile is moving in a direction perpendicular to the line joining the transmitter and the receiver ($\phi_v = 90°$). Three different radii of the scattering circle are considered here: 0.5, 1, and 1.5 kms. The Doppler spectrum of the signal at the base station using GBSBM is calculated using Eqn. 15 and the pdf $f_\phi(\phi)$ is given by Eqn. 10. The Doppler spectrum using Clarke's model is calculated using Eqn. 16. The Doppler spectra using the GBSBM and Clarke's models are compared in Figure 4. The Doppler spectrum obtained from the GBSBM model shows frequency components only around 0 Hz when $\phi_v = 90°$. This is due to the fact that the pdf of the AOA of the multipaths at the base station is nonzero only for a range of AOAs of the multipaths. The Doppler spectrum is centered around zero, because $\phi_v = 90$ degrees. The Doppler spectrum will be shifted towards the maximum Doppler frequency (f_m) if $\phi_v = 0$ or 180 degrees.

For the parameters listed in Table 1, Figures 5 and 6 show the envelopes of the fading signal obtained using Clarke's model and the GBSBM model, respectively. All the envelopes plotted are normalized by their RMS value and a value of $A_o = 1$ was used in all these simulations. It can be seen that the GBSBM model predicts that the Doppler spread is related to the radius of the scattering circle. As the radius of the scattering circle increases, the range of AOA of the multipath components increases and so does the Doppler spread. Figure 5, the fading envelope obtained from Clarke's model which is appropriate to model signal at the mobile, shows more rapid fluctuations than the envelopes in Figure 6, obtained from GBSBM model. Time axis in these figures can be thought of as distance and this explains why the spatial correlation of the signals at the base station is larger

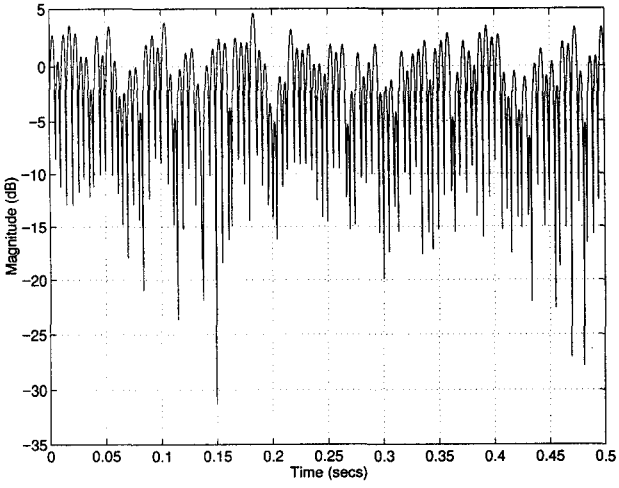

Figure 5: Fading envelopes using Clarke's model with Doppler frequency of 100 Hz. The envelope is normalized by the RMS value.

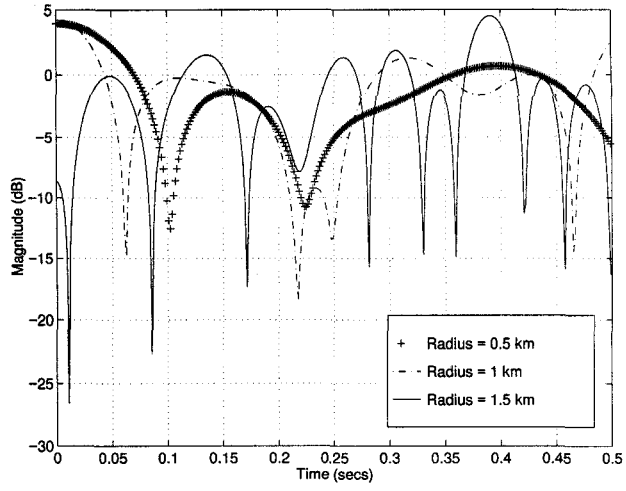

Figure 6: Fading envelopes using GBSBM model with Doppler frequency of 100 Hz with scattering circles of radii of 0.5, 1, and 1.5 km and the base station is located 10 km away from a mobile. The mobile moves in a direction which makes 90 degrees with respect to the direct path, measured clockwise. The envelopes are normalized by their RMS value.

than at the mobile unit for a fixed separation between the antenna elements. Therefore, diversity antennas at the base station must be spaced farther apart to have uncorrelated components when compared to a mobile unit.

V. Conclusions

In this paper, we have introduced a statistical geometric propagation model for a macrocell mobile environment. This channel model assumes that each multipath component of the mobile transmission undergoes only one bounce traveling from the transmitter to the receiver and the scatterers are located uniformly within a circle around the mobile. This Geometrically Based Single Bounce Macrocell (GBSBM) channel model provides three important parameters that characterize a channel: the power of the multipath component, the time-of-arrival (TOA) of the component, and the angle-of-arrival (AOA) of the components. The results show that the rate of fading at the base station is lower than at the mobile and the reduction in the rate of fading at the base station with respect to the mobile is dependent on the direction of motion of the mobile with respect to the base station and the radius of the scattering circle.

References

[1] B. G. Agee, K. Cohen, J. H. Reed, and T. C. Hsia, "Simulation performance of a blind adaptive array for realistic channels," in *Proc. IEEE Veh. Tech. Conf.*, vol. 1, pp. 97–100, 1993.

[2] J. Winters, J. Salz, and R. Gitlin, "The impact of antenna diversity on the capacity of wireless communication systems," in *IEEE Trans. on Comm.*, vol. 42, pp. 1740–1751, Feb./March/April 1994.

[3] P. Petrus and J. H. Reed, "AMPS cochannel interference rejection using spectral correlation properties and an adaptive array," in *Proc. of IEEE Veh. Tech. Conf.*, vol. 1, pp. 300-305, July 1995.

[4] R. H. Clarke, "A statistical theory of mobile-radio reception," in *Bell Syst. Tech. J.*, vol. 47, No. 6, pp. 957–1000, July-Aug 1968.

[5] T. Aulin, "A modified model for the fading signal at a mobile radio channel," in *IEEE Trans. Veh. Tech.*, vol. 28, No. 3, pp. 182–203, 1979.

[6] J. C. Liberti and T. S. Rappaport, "A geometrically based model for line-of-sight multipath radio channels," in *Proc. of IEEE Veh. Tech. Conf.*, pp. 844–848, April 1996.

[7] F. Amoroso and W. W. Jones, "Geometric model for DSPN satellite reception in the dense scatterer mobile environment," in *IEEE Trans. Comm.*, vol. 41, pp. 450–453, Mar. 1993.

[8] H. Starks and J. W. Woods, *Probability, Random variables, and Estimation Theory for Engineers.* Prentice Hall, Englewood Cliffs, 1986.

[9] J. C. Liberti, "Analysis of CDMA cellular radio systems employing adaptive antennas," in *Dissertation, Virginia Tech.*, 1995.

[10] W. C. Jakes, *Microwave Mobile Communication.* New York: Wiley, 1974.